lithium ferrite), the above mechanism can account qualitatively for the entire ΔH vs ν curve. Moreover, the T dependence in this case can be the same as in YIG since in both cases it depends essentially on the intrinsic interactions of the spin waves. Whether this is a more nearly correct picture of the relaxation process than the first mechanism[13] or, indeed, whether the degeneracy has anything at all to do with relaxation of the uniform mode in disordered ferrites might be answered by making measurements of ΔH on carefully polished samples of different shapes.

ACKNOWLEDGMENTS

The author wishes to thank V. J. Folen for the growth and x-ray analysis of the crystals and Dr. G. T. Rado for valuable discussions of this work.

PHYSICAL REVIEW VOLUME 129, NUMBER 1 1 JANUARY 1963

Hybrid Resonance and "Tilted-Orbit" Cyclotron Resonance in Bismuth

G. E. Smith, L. C. Hebel, and S. J. Buchsbaum
Bell Telephone Laboratories, Murray Hill, New Jersey
(Received 3 August 1962)

Measurements have been made of microwave absorption in very pure, single-crystal bismuth as a function of static magnetic field, **B** at 1.2°K and 70 kMc/sec. The field **B** was in the plane of the sample along a crystallographic axis; the microwave electric field **E** was either perpendicular or parallel to **B**. Except at very low magnetic fields ($\leq$100 G), nearly classical skin effect conditions prevail. Onsets of absorption are observed that result from singularities in the effective dielectric coefficient of the bismuth plasma. With **E** perpendicular to **B** most of the onsets do not correspond to any previously measured type of single-carrier cyclotron resonance in bismuth, but are hybrid resonances which require the presence of at least two distinct carriers. Such hybrid resonances are associated with longitudinal plasma modes. With **E** parallel to **B**, individual carrier cyclotron resonance is observed for those carriers whose cyclotron-orbit planes are tilted with respect to the magnetic field. Such tilts exist when **B** is not parallel to one of the major axes of the electron energy ellipsoids. A close fit to the experimental data is obtained by a theoretical calculation based on electron and hole masses measured in other experiments.

I. INTRODUCTION

CYCLOTRON resonance experiments on metals have proven a powerful tool for determining the effective masses of carriers and their mass anisotropy. So far, two geometries have been utilized in such experiments: The Galt geometry[1] and the Azbel'-Kaner geometry.[2] In the Galt geometry the static magnetic field is applied perpendicular to the surface of the sample, and absorption (or reflection) of circularly polarized radiation that is incident normally on the sample (i.e., along the magnetic field) is measured. By this method it is possible to determine both the effective mass of the carrier and the sign of its charge. This method was used extensively for bismuth under classical skin conditions.[1,3]

In the Azbel'-Kaner geometry the static magnetic field is applied in the plane of the sample and the surface impedance is measured for normally incident radiation that is linearly polarized either parallel or perpendicular to the static magnetic field. Many experiments have been carried out under anomalous skin conditions; the surface resistance then exhibits oscillations with maxima at harmonics of the carrier frequency and yields the mass of the carriers but not the sign of the charge.

In this paper we report experiments on bismuth in an Azbel'-Kaner type geometry but under nearly classical skin effect conditions. In the experiment the plasma frequency of the carriers is much larger than the radiation frequency and the microwave electric field **E** was either perpendicular or parallel to the static magnetic field **B**. As is shown in detail in Sec. II, when **E** is perpendicular to **B** and the mass of the carriers is isotropic, cyclotron resonance of individual carriers is shielded out by the large longitudinal depolarizing fields,[4] which strongly couple the longitudinal and transverse degrees of freedom of the plasma and shift the nautral frequencies of the plasma away from the cyclotron frequencies. When two or more carriers of distinct charge-to-mass ratios are present in a high-density plasma, all but one of the shifted frequencies become hybrid frequencies which involve the masses of all carriers. The remaining resonant frequency is near

[1] J. K. Galt, W. A. Yager, F. R. Merritt, B. B. Cetlin, and A. D. Brailsford, Phys. Rev. **114**, 1396 (1959).
[2] M. Ya. Azbel' and E. A. Kaner, Soviet Phys.—JETP **3**, 772 (1956); as an experimental example, see A. F. Kip, D. N. Langenberg, and T. W. Moore, Phys. Rev. **124**, 359 (1961); J. E. Aubrey and R. G. Chambers, J. Phys. Chem. Solids **3**, 128 (1957).
[3] Preliminary experiments already reported [J. K. Galt, F. R. Merritt, and P. H. Schmidt, Phys. Rev. Letters **6**, 458 (1961); J. K. Galt, F. R. Merritt, W. A. Yager, and H. W. Dail, Jr., *ibid.* **2**, 292 (1959)] and additional experiments under way [J. K. Galt (private communication)] indicate that the method is also applicable to metals in which anomalous skin effect conditions exist.
[4] P. W. Anderson, Phys. Rev. **100**, 749 (1955).

the plasma frequency. Such hybrid resonances have been observed in gaseous[5] and in semiconductor[6] plasmas. When the carriers possess anisotropic masses there may also exist singularities at the cyclotron frequencies of such carriers.

When $\mathbf{E}$ is parallel to $\mathbf{B}$, individual carrier cyclotron resonance is observed for carriers whose orbits are tilted with respect to the magnetic field.

In Sec. II we review the theory of hybrid resonances for the simple case of a plasma with isotropic carriers and infinite relaxation times. Resonance in a plasma with anisotropic carriers is discussed in Sec. III. In Sec. IV we describe the experimental method. In Sec. V we present the experimental results and compare them with calculations based on the known band structure of bismuth. Finally, a summary and conclusions are presented in Sec. VI.

II. HYBRID RESONANCE IN A PLASMA WITH ISOTROPIC CARRIERS

When a plasma possesses more than two distinct type carriers with anisotropic masses the general expression for the absorption of microwave radiation by the plasma in the Azbel'-Kaner geometry is sufficiently involved that it is constructive to consider first the academic case of a uniform plasma with only two carriers with isotropic masses and infinite relaxation times. Such isotropic models have been discussed for gaseous plasmas[7] and for metals.[8] We take the carriers to be electrons of density n, mass m_e and holes of density n, mass m_h. Under classical skin-effect conditions it is adequate to neglect the effect of carrier random velocity in the Fermi sea and to describe the motion by the Lorentz force equation

$$m_{e,h}(\partial \mathbf{v}_{e,h}/\partial t)=\pm e[\mathbf{E}+\mathbf{v}_{e,h}\times\mathbf{B}], \tag{1}$$

where $\mathbf{E}$ is the total, self-consistent microwave electric field in the plasma ($\mathbf{E}\sim\mathbf{E}_1 \exp j\omega t$), and $\mathbf{B}$ is the applied static magnetic field. Equation (1) gives the ordered velocity, $\mathbf{v}_{e,h}$, of electrons and holes from which the conduction current, $\mathbf{J}=ne(\mathbf{v}_h-\mathbf{v}_e)=\boldsymbol{\sigma}\cdot\mathbf{E}$, and thus the plasma conductivity $\boldsymbol{\sigma}$ can be obtained. Because of the presence of the static magnetic field $\mathbf{B}$, $\boldsymbol{\sigma}$ is generally a tensor. It is convenient to define an effective dielectric tensor of the plasma by

$$\boldsymbol{\varepsilon}=\epsilon_l\mathbf{I}+\boldsymbol{\sigma}/j\omega\epsilon_0, \tag{2}$$

where ϵ_l is the lattice dielectric constant, $\mathbf{I}$ is unit tensor, and ϵ_0 is the permittivity of free space. Mks units will be used throughout.

[5] S. J. Buchsbaum, Phys. Rev. Letters **5**, 495 (1960).
[6] R. E. Michel and B. Rosenblum, Phys. Rev. Letters **7**, 234 (1961).
[7] K. Körper, Z. Naturforsch, **a12**, 815 (1957); P. L. Auer, H. Hurwitz, Jr., and R. D. Miller, Phys. Fluids **1**, 501 (1958); S. J. Buchsbaum, *ibid* **3**, 418 (1960).
[8] B. Lax and J. G. Mavroides, in *Solid State Physics*, edited by F. Seitz and D. Turnbull (Academic Press Inc., New York, 1960), Vol. XI, p. 261.

For the simple case considered and when $\mathbf{B}$ is uniform and is oriented along the z axis of a Cartesian coordinate system, $\boldsymbol{\varepsilon}$ has the form

$$\boldsymbol{\varepsilon}=\begin{vmatrix}\epsilon_\perp & -\epsilon_\times & 0\\ \epsilon_\times & \epsilon_\perp & 0\\ 0 & 0 & \epsilon_{\parallel}\end{vmatrix}, \tag{3}$$

$$\epsilon_\perp=\epsilon_l-\frac{\omega_{pe}^2}{\omega^2-\omega_{ce}^2}-\frac{\omega_{ph}^2}{\omega^2-\omega_{ch}^2},$$

$$\epsilon_\times=j\frac{\omega_{pe}^2}{\omega^2-\omega_{ce}^2}\frac{\omega_{ce}}{\omega}-j\frac{\omega_{ph}^2}{\omega^2-\omega_{ch}^2}\frac{\omega_{ch}}{\omega},$$

$$\epsilon_{\parallel}=1-\frac{\omega_{pe}^2}{\omega^2}-\frac{\omega_{ph}^2}{\omega^2}=1-\frac{\omega_p^2}{\omega^2},$$

where $\omega_{ce}=eB/m_e$ and $\omega_{ch}=eB/m_h$ are the electron and hole cyclotron frequencies, $\omega_{pe}=(ne^2/m_e\epsilon_0)^{1/2}$ and $\omega_{ph}=(ne^2/m_h\epsilon_0)^{1/2}$ are the electron and hole plasma frequencies, and $\omega_p=[ne^2(m_e+m_h)/(m_em_h\epsilon_0)]^{1/2}$ is the total plasma frequency.

The use of Maxwell's equations then leads to the wave equation

$$\nabla\times\nabla\times\mathbf{E}-(\omega^2/c^2)\boldsymbol{\varepsilon}\cdot\mathbf{E}=0, \tag{5}$$

from which the self-consistent field $\mathbf{E}$ must be obtained.

For a plane wave of the form $\mathbf{E}\sim\mathbf{E}\exp j(\omega t-\mathbf{k}\cdot\mathbf{r})$ Eq. (5) constitutes three simultaneous homogeneous equations for the three Cartesian components of $\mathbf{E}$. For a nontrivial solution, the determinant of the coefficients must vanish, and this constitutes the dispersion relation. Our experimental conditions are such that within the plasma a plane wave of the form $\mathbf{E}=\mathbf{E}\exp j(\omega t-kx)$ propagates in the positive x direction at right angles to the static magnetic field which is oriented in the positive z direction. For this form of the field, the dispersion relation is

$$[k^2-(\omega^2/c^2)\epsilon_{\parallel}][k^2\epsilon_\perp-(\epsilon_\perp^2+\epsilon_\times^2)\omega^2/c^2]=0. \tag{6}$$

The dispersion equation is biquadratic in k^2, indicating that, in general, two waves of different propagation vectors $\mathbf{k}$ can exist in the plasma. We shall denote the two roots k_0 and k_e, where

$$k_0^2=(\omega^2/c^2)\epsilon_{\parallel}, \tag{7}$$

and

$$k_e^2=(\omega/c)^2(\epsilon_\perp^2+\epsilon_\times^2)/\epsilon_\perp. \tag{8}$$

An examination of the cofactors of Eq. (5) reveals that the root k_0 corresponds to the ordinary wave, that is, the wave polarized along the static magnetic field, $\mathbf{E}=(0,0,E_z)$. In our experiment $\omega^2\ll\omega_p^2$, $k_0^2=(\omega^2/c^2)(1-\omega_p^2/\omega^2)$ is a large negative quantity; thus, the wave is cut off, and nearly total reflection is expected for all values of the magnetic field when such a wave incident on a semi-infinite sample from the left.

This conclusion no longer holds when the carriers possess anisotropic masses such that the plane of the carrier orbit is not at right angles to the magnetic field. Then absorption at cyclotron resonance of individual carriers takes place, as is shown in detail in Sec. V. We call such resonance "tilted-orbit" cyclotron resonance. Such resonance was discussed for semiconductors by Shockley and by Lax *et al.*[9]

The more interesting wave is the extraordinary wave. It corresponds to the root k_e. For this wave, the E field is of the form $\mathbf{E}=(E_x,E_y,0)$, where

$$E_x/E_y=\epsilon_\times/\epsilon_\perp. \tag{9}$$

As $\epsilon_\times$ is imaginary, this wave is elliptically polarized in the plane transverse to $\mathbf{B}$. Note, that E_x is finite so that the wave is partially longitudinal and partially transverse. It is the presence of the longitudinal electric field with its associated space charge that shields out cyclotron resonance when $\omega_p^2\gg\omega^2$.[4] This follows from Eq. (9) and (4) which give

$$\begin{aligned}\frac{E_x}{E_y}&=\frac{E_{\text{longitudinal}}}{E_{\text{transverse}}}=\frac{\epsilon_\times}{\epsilon_\perp}=j\frac{\omega_{ce}(\omega^2-\omega_{ch}^2)\omega_{pe}^2-\omega_{ch}(\omega^2-\omega_{ce}^2)\omega_{ph}^2}{\omega[(\omega^2-\omega_{ce}^2)(\omega^2-\omega_{ch}^2)\epsilon_l-\omega_{pe}^2(\omega^2-\omega_{ch}^2)-\omega_{ph}^2(\omega^2-\omega_{ce}^2)]}\\&=-j\quad\text{when}\quad\omega=\omega_{ce}\\&=+j\quad\text{when}\quad\omega=\omega_{ch}.\end{aligned} \tag{10}$$

Thus, at $\omega=\omega_{ce}$ (electron cyclotron resonance) the electric field is circularly polarized, but it rotates in the sense opposite to that of the electrons in the plasma. The same is true at $\omega=\omega_{ch}$ (hole cyclotron resonance); that is, the field is circularly polarized but rotates in the sense opposite to that of the holes. As a result, no resonant absorption exists at either cyclotron frequency. Nevertheless, there exists a resonance condition and it obtains from Eq. (8):

$$k_e^2=\frac{\omega^2}{c^2}\left[\epsilon_l-\frac{\omega_p^2(\omega^2-\bar{\omega}_p^2-\omega_{ce}\omega_{ch})}{(\omega^2-\omega_{ce}^2)(\omega^2-\omega_{ch}^2)-\bar{\omega}_p^2(\omega^2-\omega_{ce}\omega_{ch})}\right], \tag{11}$$

where $\bar{\omega}_p^2=\omega_p^2\epsilon_l$. The propagation constant k_e becomes infinite (or, in presence of collisional damping, large) at a frequency given by

$$D(\omega)=(\omega^2-\omega_{ce}^2)(\omega^2-\omega_{ch}^2)-\bar{\omega}_p^2(\omega^2-\omega_{ce}\omega_{ch})=0. \tag{12}$$

Under the conditions of our experiment ($\omega_p^2\gg\omega^2$), the roots of Eq. (12) are very nearly

$$\omega=\bar{\omega}_p \tag{13a}$$

and

$$\omega=(\omega_{ce}\omega_{ch})^{1/2}. \tag{13b}$$

The root $\omega=\omega_p$ corresponds to the oscillation of electrons and holes out of phase with each other; it is not accessible in our experiment. The root $\omega=(\omega_{ce}\omega_{ch})^{1/2}$ is accessible. It is the so-called electron-hole hybrid frequency which has been studied extensively in gaseous plasmas.[7,5] At this frequency $E_x/E_y\to\infty$, so the field is very nearly linearly polarized in the longitudinal direction. It represents a transition condition from left- to right-rotating elliptic polarization as the frequency is varied from the electron cyclotron frequency to the hole cyclotron frequency. At the electron-hole hybrid frequency the electrons and holes oscillate jointly in the longitudinal direction with only a small slippage between them; there results a much smaller space charge field than at the plasma frequency.

A degenerate situation exists when the electron and hole masses are identical. Equation (11) becomes

$$k_e^2=\frac{\omega^2}{c^2}\left[\epsilon_l-\frac{\omega_p^2}{\omega^2-\omega_c^2}\right], \tag{14}$$

where $\omega_c=\omega_{ce}=\omega_{ch}$. There is a resonance at $\omega=\omega_c$; but it is not a hybrid resonance because when $m_e=m_h$, the electron and hole velocities along k are identical. Consequently, although there is mass motion in the longitudinal direction, there is no current; $\epsilon_\times\equiv0$, and thus no space-charge field exists.

The experimental procedure consists of varying the surface reflection coefficient, R, with the magnetic field B; the measured quantity is the absorption coefficient A which is $(1-R)$ for a sufficiently thick medium. For normal incidence on a semi-infinite plasma,

$$A=4\,\text{Re}\eta/|1+\eta|^2, \tag{15}$$

where η, the complex index of refraction, is given by $\eta^2=c^2k^2/\omega^2$. For $\omega_p^2\gg\omega^2$, $|\eta|\gg1$ and to good approximation

$$A=4/\text{Re}\eta. \tag{16}$$

Since in this limit

$$\eta^2\cong-\omega_p^2/(\omega^2-\omega_{ce}\omega_{ch}), \tag{17}$$

hybrid resonance manifests itself as an onset of absorption, as is shown schematically in Fig. 1. Note that at large magnetic fields, $\omega_{ce}\omega_{ch}>\omega^2$, absorption is directly proportional to the magnetic field. In this region the wave in the plasma is the extraordinary Alfvén wave.[10]

When the plasma possesses p distinct carriers of different charge-to-mass ratios, $(p-1)$ distinct hybrid frequencies exist. For example, for two kinds of electrons of isotropic masses m_1 and m_2 and cyclotron frequencies $\omega_{c1}=eB/m_1$ and $\omega_{c2}=eB/m_2$, and one type of

[9] W. Shockley, Phys. Rev. **90**, 491 (1953); B. Lax, H. J. Zeiger, and R. N. Dexter, Physica **20**, 818 (1954).

[10] S. J. Buchsbaum and J. K. Galt, Phys. Fluids **4**, 1514 (1961).

hole of isotropic mass m_h and cyclotron frequency $\omega_{ch}=eB/m_h$, the denominator in Eq. (11) has the form[7]

$$D(\omega)=(\omega^2-\omega_{c1}^2)(\omega^2-\omega_{c2}^2)(\omega^2-\omega_{ch}^2) -\bar{\omega}_p^2(\omega^2-\omega_{h1}^2)(\omega^2-\omega_{h2}^2), \quad (18)$$

where the two hybrid frequencies ω_{h1} and ω_{h2} involve the cyclotron frequencies and the relative concentrations of the three carriers but not their absolute densities. One of the hybrids, say, ω_{h1} results from the oscillation of the two electronic charge clouds out of phase with one another, the holes playing a relatively minor role; this hybrid will be called the electron-electron hybrid. The other hybrid results from a joint oscillation of holes and electrons with a small slippage between the positive and negative carriers, and will be called the electron-hole hybrid.

When the plasma consists of two types of electrons and one type of hole, the behavior of η^2 and of the absorption coefficient, A, with B is depicted schematically in Fig. 2. The two hybrid resonances (the infinities in η^2) manifest themselves as onsets of absorption, while the zero of η^2, the so-called dielectric anomally,[11] manifests itself as a virtually discontinuous decrease in absorption. At very large magnetic field, absorption is again proportional to B and can be described in terms of the properties of an Alfvén wave.

III. RESONANCE IN A PLASMA WITH ANISOTROPIC CARRIERS

As was shown in Eq. (10) and in the discussion that followed it, in a high-density plasma composed of isotropic carriers, cyclotron resonance of individual carriers is shielded out by the space charge fields which cause the total electromagnetic field in the plasma to be of the wrong polarization to excite cyclotron resonance in the extraordinary wave. Can the plasma achieve such shielding for anisotropic carriers? If all carriers of a given cyclotron mass m^* are given by a single mass tensor, the answer is yes. At $\omega=eB/m^*$ sufficient space charge field is induced so that there exists within the plasma an electromagnetic field which is precisely orthogonal to that required to excite cyclotron resonance. This is shown in detail in Appendix A. However, when the anisotropic carriers of a given cyclotron mass m^* are distributed among two (or more) nonequivalent mass tensors (as for example, when the cyclotron orbits are two sets of ellipses with their major axes not parallel) the polarization of the "normal-mode" field for excitation of cyclotron resonance is different for each of the mass tensors. Thus, the plasma cannot produce adequate space charge field that is orthogonal to both such "normal modes." As a consequence, in addition to any hybrid resonance that may exist because of the presence of carriers of other cyclotron masses, the extraordinary wave also will exhibit cyclotron resonance of the carrier in question as shown in Appendix A.

As will be shown in detail in Sec. V a clear-cut example in bismuth of inadequate shielding at electron cyclotron resonance occurs when the static magnetic field B is along the threefold axis of symmetry of the crystal. An example of complete shielding at the electron cyclotron resonance in the presence of two equivalent mass ellipsoids occurs for B along the twofold axis of symmetry.

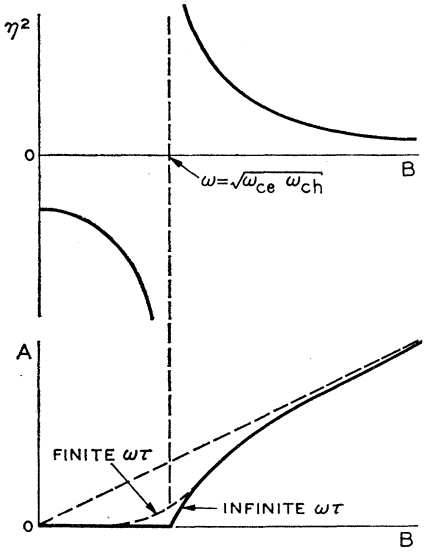

FIG. 1. Schematic plot of the squared index of refraction and of the absorption coefficient as a function of magnetic field in the presence of an electron-hole hybrid resonance $\omega=(\omega_{ce}\omega_{ch})^{1/2}$.

[11] W. S. Boyle, A. D. Brailsford, and J. K. Galt, Phys. Rev. **109**, 1396 (1958).

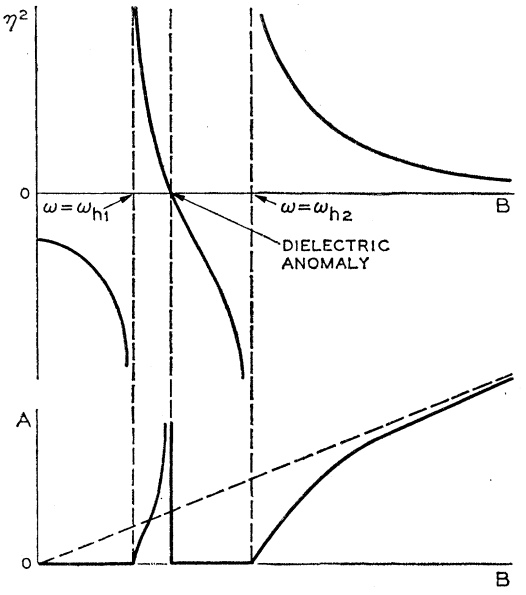

FIG. 2. Schematic plot of the squared index of refraction and of the absorption coefficient as a function of magnetic field in the presence of two hybrid resonances, $\omega=\omega_{h1}$ and $\omega=\omega_{h2}$.

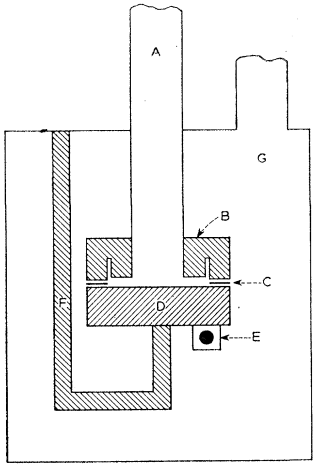

FIG. 3. Schematic drawing of the apparatus.

IV. EXPERIMENTAL METHOD

To obtain the large values of $\omega\tau$ needed for sharp resonances, the experiment was carried out on high-purity bismuth at 70 kMc/sec and 1.2°K. Single crystals were grown by the pulling technique from zone-refined bismuth available commercially and stated to be pure to 1 part in 10^6. After orientation by Laue x-ray photographs, slabs approximately $\frac{1}{8}$ in. thick were cut by an acid-string saw and the surfaces acid lapped flat using concentrated nitric acid on twill jean cloth. All samples were cut with one of its principal axes perpendicular to the surface of the slab. Squares, 0.32 in. by 0.32 in., were cut from the slabs with their sides oriented along principal axes of the crystal, and one surface of the square was electropolished.[12] The resulting surface was flat on a macroscopic scale to better than 0.001 in. The orientation of principal axes with respect to the sides of the sample was accurate to within 2°.

The method of measuring microwave absorption is similar to the calorimetric technique used by Fawcett[13] and is shown in Fig. 3. The sample D is placed at the end of a nonresonant rectangular microwave line A leading into a vacuum space G. The sample is thermally insulated from the line by 0.001-in. mica spacers C; a choke flange B is used to prevent microwave leakage through this space. The sample was lightly spring loaded against the flange and connected to the helium bath by a heat leak F. The sample temperature is measured by a carbon thermometer E. When the microwave power is turned on, there is a temperature rise in the sample which is directly proportional to the power absorption. The microwaves are modulated at 13 cps, and a 13-cps signal is detected across the dc-biased carbon thermometer. The thermal time constant of the sample and the heat leak is about 1 sec. The ac method minimizes errors due to drift and allows continuous detection as the magnetic field is swept. The noise-to-signal ratio was about 1%, and within a single run the results were reproducible to within 3%.

The quantity measured experimentally was the ratio $A(B)/A(0)$, where $A(B)$ is the absorption coefficient at a magnetic field value B. To obtain absolute magnitudes, measurements[12] of $A(0)$ at 24 kMc/sec were scaled up by $\omega^{2/3}$ to give values of $A(0)$ at 70 kMc/sec. Scaling by $\omega^{2/3}$ assumes that anomalous skin effect conditions prevail at zero field. This assumption will be discussed in greater detail in the conclusions.

Bismuth has a crystal structure which can be described by a rhombohedral unit cell containing two atoms.[14] A Cartesian coordinate system is chosen in which axis 1 lies along the binary axis; axis 2 along the bisectrix axis; and axis 3 along the trigonal axis; that is, there is 180° rotational symmetry about axis 1, 120° rotational symmetry about axis 3, and axes 2 and 3 lie in a reflection plane. Since bismuth is highly anisotropic, care had to be taken to minimize misorientation errors. One side of the sample was oriented perpendicular to the microwave E field by a line-up block (not shown in Fig. 3) which was accurately parallel to the broad side of the rectangular waveguide. The resulting accuracy in aligning a side of the sample along the microwave field is estimated to be within 2°. The magnetic field could be rotated in the plane of the sample, allowing orientation of the magnetic field along a principal axis when there are reflection symmetries as a function of magnetic field angle. This could be done for rotations in the plane formed by the trigonal and binary axes, where there is reflection symmetry about the trigonal axis and in the binary-bisectrix plane, where there is a reflection symmetry about the bisectrix axis. Such alignment could be done to within 1°. The bisectrix-trigonal plane, however, has no reflection symmetry, and the error in mechanical alignment of the waveguide with respect to the field was estimated to be within 3°. Orientation of the plane of rotation of the magnetic field to the plane of the sample was accurate to within 2°. To check reproducibility, two samples were made of each of the three principal orientations. The positions of the observed maxima and minima in absorption in the two samples generally agreed, but the amplitudes significantly varied.

V. RESULTS AND ANALYSIS

The calculations are based on the model of the band structure which has been used previously to interpret de Haas–van Alphen, transport, and cyclotron resonance experiments on bismuth.[14] The electron band is made up of three ellipsoids slightly tilted out of the plane perpendicular to the threefold axis; for a typical ellipsoid the electron energy, referred to an origin at its center, is given by

$$E=(\hbar^2/2m_0)(\alpha_1 k_1^2+\alpha_2 k_2^2+2\alpha_4 k_2 k_3+\alpha_3 k_3^2), \quad (19)$$

[12] G. E. Smith, Phys. Rev. **115**, 1561 (1959).
[13] E. Fawcett, Proc. Roy. Soc. (London) **A232**, 519 (1955).
[14] W. S. Boyle and G. E. Smith, in *Progress in Semiconductors* (Heywood & Company, Ltd. London, to be published), Vol. 7.

where k_1, k_2, and k_3 are the wave vector components parallel to the binary, bisectrix and trigonal axes: m_0 is the free electron mass and the α's are components of the reciprocal mass tensor. For such an ellipsoid, called ellipsoid a, the effective mass tensor has the form

$$\mathfrak{m}_a = m_0 \begin{bmatrix} m_1 & 0 & 0 \\ 0 & m_2 & m_4 \\ 0 & m_4 & m_3 \end{bmatrix}, \tag{20}$$

where m_1, m_2, m_3, and m_4 are effective masses in units of m_0. The remaining ellipsoids, ellipsoids b and c, are obtained by rotations of the ellipsoid a through $\pm 120°$ about the trigonal axis.

The hole band is made up of an ellipsoid of revolution about the trigonal axis. For the holes,

$$E - E_b = (\hbar^2/2m_0)(k_1^2/M_1 + k_2^2/M_1 + k_3^2/M_3), \tag{21}$$

where E_b is the band overlap energy and M_1 and M_3 are the effective masses in units of m_0.

The conductivity tensor for this model has been calculated[15] assuming separate, isotropic relaxation times for electrons and holes. The current $\mathbf{J}$ for each type carrier is calculated using

$$\mathfrak{m} \cdot d\mathbf{J}/dt + \mathfrak{m} \cdot \mathbf{J}/\tau = ne^2\mathbf{E} + e\mathbf{J} \times \mathbf{B}, \tag{22}$$

where $\mathfrak{m}$ is the effective-mass tensor, τ is the relaxation time for the carrier, $\mathbf{E}$ and $\mathbf{B}$ are the microwave electric and static magnetic fields, respectively, and n is the carrier density.

The total conductivity tensor $\boldsymbol{\sigma}$ is the sum of the electron and hole tensors. The components of the effective dielectric tensor $\boldsymbol{\varepsilon}$ are then given by Eq. (2). Using the dielectric tensor, we have made a calculation based on Eq. (5), of the power absorption versus B with the aid of an IBM 7090 computer. The components of the conductivity and dielectric tensors as well as the appropriate equations for power absorption will be given below for each orientation of $\mathbf{B}$ relative to the three principal crystal axes. The following parameters gave the best fit with experimental curves: $m_1 = 0.0062$, $m_2 = 1.30$, $m_3 = 0.017$, $m_4 = -0.085$; $M_1 = 0.057$, $M_3 = 0.77$, the electron and hole densities, $n = 2.3 \times 10^{17}/\text{cm}^3$; and $\epsilon_l = 100$. The merits of the choice of parameters will be discussed further in the conclusions.

Curves of power absorption coefficients A versus static field B are presented in Figs. 4 through 13 for six orientations with $\mathbf{E}$ perpendicular to $\mathbf{B}$ and six with $\mathbf{E}$ parallel to $\mathbf{B}$: Measurements were taken to 17 kG in all cases. The main features of the curves are explained in terms of the hybrid resonances and "tilted-orbit" cyclotron resonances previously outlined. It will be noted that additional singularities are evident in the absorption which have been tentatively identified as spin resonance and combination resonance[16]; such singularities will not be discussed in detail in this paper. Although these resonances are generally smaller in amplitude than the hybrid resonances, their presence significantly alters the apparent line shape near the onsets of absorption at hybrid resonances. At fields below a few hundred gauss, the cyclotron radius in comparable to or larger than the skin depth and a small amplitude Azbel'-Kaner effect is observed for most orientations. The scale of the experimental plots used here to display hybrid resonances is too small to show these clearly.

The theoretical curves shown in the figures were calculated with $\omega\tau_e = 6$ and $\omega\tau_h = 15$, which gave a compromise fit for all curves. It is a common feature of almost all the curves that the choice of longer relaxation times would improve the shape of the absorption curves in some regions but would result in calculated heights of some absorption peaks being much higher than observed values. As will be discussed further in the conclusions, the agreement between theory and experiment is best when the absorption is large; under such circumstances the skin depth is long, so that one would expect the skin-effect conditions to become classical, as assumed in the theory.

A. B Parallel to Trigonal Axis

For this orientation all electron ellipsoids yield the same cyclotron mass, but the major axes of their cyclotron orbits are inclined at 120° to each other. Labeling the binary, bisectrix, and trigonal axes as axis 1, axis 2, and axis 3, respectively, the conductivity tensor for electrons has the following components[15]:

$$\sigma_{11}/\sigma_0 = \sigma_{22}/\sigma_0 = (1/2\Delta)[(m_1 + m_2)m_3 - m_4^2], \tag{23a}$$

$$\sigma_{12}/\sigma_0 = -\sigma_{21}/\sigma_0 = bm_3/\Delta, \tag{23b}$$

$$\sigma_{33}/\sigma_0 = (1/\Delta)(m_1 m_2 + b^2), \tag{23c}$$

$$\Delta = m_1(m_2 m_3 - m_4^2) + m_3 b^2, \tag{24a}$$

$$\sigma_0 = ne^2/[m_0(j\omega + 1/\tau)], \tag{24b}$$

$$b = eB/[m_0(j\omega + 1/\tau)], \tag{24c}$$

where n is the electron density, m_0 the free electron mass, $1/\tau$ the collision frequency, and ω is the angular frequency of the microwave field.

The corresponding conductivity tensor components for the holes can be obtained from Eq. (23) and (24) using hole masses and changing the sign of b.

For a plane polarized wave incident normally to the sample, solution of Eq. (5) using Eqs. (2), (23), and (24) shows that the normal modes for $\mathbf{B}$ parallel to axis 3 have $\mathbf{E}$ in the incident wave polarized either parallel or perpendicular to $\mathbf{B}$. Writing the complex index of refraction as η, the power absorbed is given by

$$A = 4\,\text{Re}\eta/|1+\eta|^2. \tag{25}$$

[15] B. Lax, K. J. Button, H. J. Zeiger, and Laura M. Roth, Phys. Rev. 102, 715 (1956).

[16] G. E. Smith, J. K. Galt, and F. R. Merritt, Phys. Rev. Letters 4, 276 (1960).

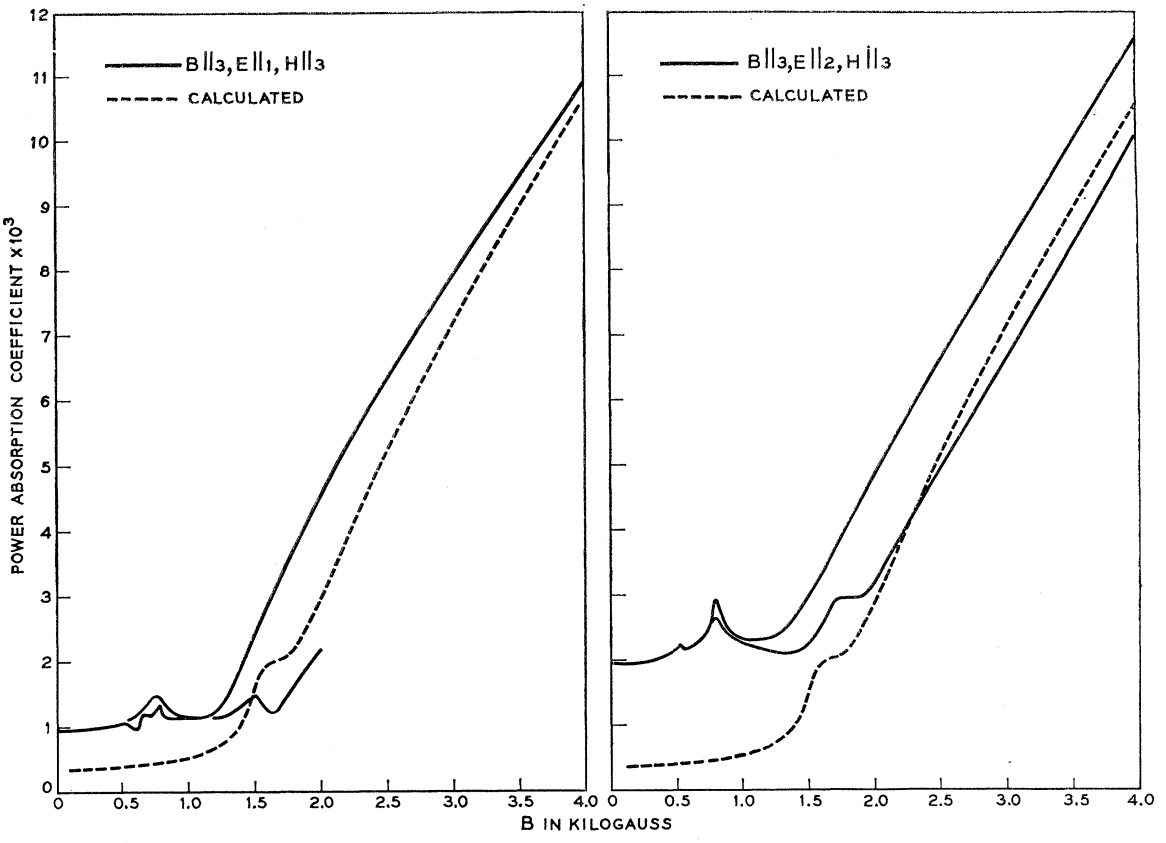

FIG. 4. Theoretical and experimental plots of power absorption coefficient as a function of magnetic field; **B** is along the trigonal axis and E and H refer to the polarization of the incident microwave field. Experimental curves from two different samples are shown in each figure to exhibit the sensitivity to slight sample orientation errors.

(a.) For **E** perpendicular to **B**, η is independent of the polarization of **E** in the (1,2) plane since $\sigma_{11}=\sigma_{22}$.

$$\eta^2=\epsilon_{11}-\epsilon_{12}\epsilon_{21}/\epsilon_{22}. \tag{26}$$

The ratio of longitudinal to transverse fields is given by

$$E_x/E_y=\epsilon_{12}/\epsilon_{11}=-\epsilon_{21}/\epsilon_{22}. \tag{27}$$

Since the electron ellipsoids yield the same cyclotron mass but nonequivalent orbits, there exists an electron cyclotron resonance in addition to the hybrid resonance. There exists no resonance at the hole cyclotron frequency. The plot of η^2 vs B and the corresponding power absorption for $\omega\tau=\infty$ are topologically similar to those of Fig. 2.

The experimental and calculated curves are shown in Fig. 4. The hybrid resonance occurs at about 1.45 kG and the electron cyclotron resonance at about 1.9 kG. The dielectric anomaly between them is obscured by the finite $\omega\tau$. As can be noted from Fig. 4, the cyclotron resonance at 1.9 kG is very sensitive to orientation. When the static magnetic field is turned slightly from the trigonal direction, the cyclotron masses for the three electron ellipsoids become distinct, the plasma shielding becomes completely effective, and the cyclotron resonance disappears. Figure 4 is a good example of the calculated low-field absorption being lower than the observed absorption because of the anomalous skin effect. Agreement becomes better as the absorption and magnetic field increase making the medium more classical. As with all orientations, measurements were taken to 17 kG but only the low-field portions containing significant structure are presented. In the hybrid resonance geometry, the absorption in the high-field region increases linearly with B and extrapolates through the origin, as predicted theoretically.

(b.) For **E** parallel to **B**, the power absorption is again given by Eq. (25), where η is given by

$$\eta^2=\epsilon_{33}. \tag{28}$$

For this mode there is current only parallel to **B**. Thus, there are no longitudinal fields and no hybrid resonances. However, there is a resonance at the electron cyclotron frequency which may be simply interpreted.

If **B** is parallel to a major axis of the energy ellipsoid for a given type of carrier, the contribution of that type of carrier to ϵ_{33} is independent of B for **E** parallel to **B**. However, if **B** is not parallel to a major axis, the orbits for that type of carrier are "tilted" with respect to **B**; thus, there is a component of **E** in the plane of the orbit of the electrons, which results in cyclotron resonance

for that type of carrier.[9] We shall call such resonance "tilted-orbit" cyclotron resonance.

Such is the case for the electrons with **B** parallel to axis 3 because the electron ellipsoids are "tilted" out of the trigonal plane ($m_4 \neq 0$); for $\omega\tau = \infty$,

$$\frac{\epsilon_{33}}{\epsilon_0} = 1 - \frac{\omega_p^2}{\omega^2}\left[\frac{m_1 m_2 - \omega_c^2/\omega^2}{m_1(m_2 m_3 - m_4^2) - m_3\omega_c^2/\omega^2} + \frac{1}{M_3}\right], \quad (29)$$

where ω_p and ω_c are the plasma and cyclotron frequencies for a free electron mass. Equation (29) and the corresponding power absorption are plotted in Fig. 5. The resonance occurs at the electron cyclotron frequency, that is, for

$$eB/m_0 = \omega_c = \omega[m_1(m_2 m_3 - m_4^2)/m_3]^{1/2}. \quad (30)$$

Since the hole ellipsoids are not tilted out of the (1,2) plane, there is no resonance at the hole cyclotron frequency for **E** parallel to **B**.

From Fig. 5 one should note that the resonance is followed closely by a dielectric anomaly as B is increased, so that power absorption becomes small for higher fields. This is in contrast to the situation in which **E** is perpendicular to **B** where the power absorption increases on the high-field side of a resonance. (See Part II.) The shape of the power absorption curve when **E** is parallel to **B** is very sensitive to the size of m_4 relative to the other mass components.

The experimental and calculated curves for **E** parallel to **B** are presented in Fig. 6. Since only ϵ_{33} is involved, the calculated curve is the same whether axis 1 or axis 2 is perpendicular to the surface of the sample. The onset of the cyclotron resonance absorption is obscured by other resonances, but the main peak occurs at 2.15 kG for both experimental orientations, and the calculated peak is at 2.25 kG. The height of the calculated absorption peak is significantly lower than the observed peak, and a factor of two increase in relaxation times is needed to make the amplitudes agree. However, the spin resonance lines for this orientation occur at 1.7 kG for the holes and 2.0 kG for the electrons and add to the apparent height of the cyclotron resonance absorption.

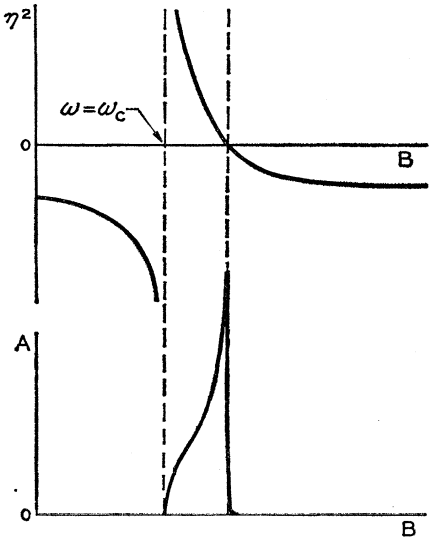

FIG. 5. Schematic plot of the squared index of refraction and of the absorption coefficient as a function of magnetic field in the presence of a "tilted-orbit" cyclotron resonance. It can be easily shown that the point $\eta^2 = 0$ always occurs at a field that is larger then the cyclotron field.

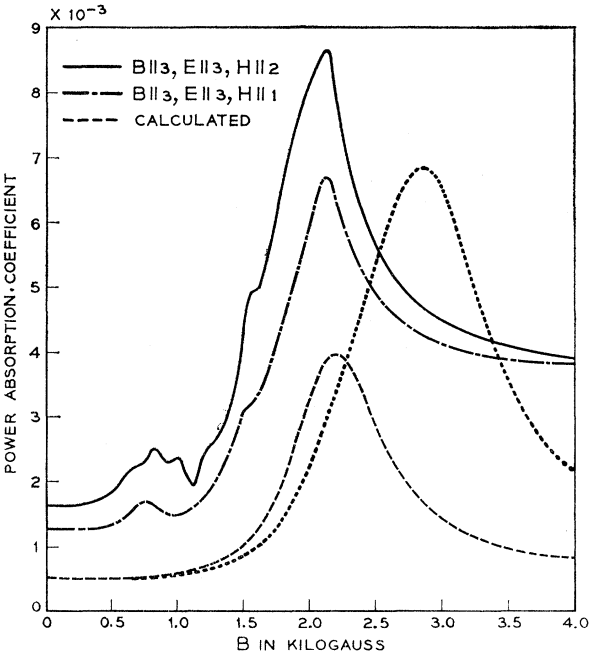

FIG. 6. Theoretical and experimental plots of power absorption coefficient as a function of magnetic field; **B** is along the trigonal axis and E and H refer to the polarization of the incident microwave field. The dotted curve was calculated using the electron masses quoted in reference 19 and the hole masses in reference 1.

B. B Parallel to Binary Axis

For this orientation electron ellipsoids b and c yield the same cyclotron mass but have equivalent orbits; ellipsoid a has a distinct cyclotron mass. The conductivity tensor for electrons has the following components[15]:

$$\frac{\sigma_{11}}{\sigma_0} = \frac{1}{3m_1} + \left(\frac{2}{3\Delta_c}\right)\left[\frac{(3m_1+m_2)m_3 - m_4^2}{4} + b^2\right], \quad (31a)$$

$$\frac{\sigma_{22}}{\sigma_0} = \frac{m_1 m_3}{3\Delta_a} + \left(\frac{2}{3\Delta_c}\right)\left[\frac{(m_1+3m_2)m_3 - 3m_4^2}{4}\right], \quad (31b)$$

$$\frac{\sigma_{33}}{\sigma_0} = \frac{m_1 m_2}{3\Delta_a} + \frac{2m_1 m_2}{3\Delta_c}, \quad (31c)$$

$$\frac{\sigma_{23}}{\sigma_0} = \frac{m_1(b - m_4)}{3\Delta_a} + \left(\frac{2}{3\Delta_c}\right)\left[\frac{(m_1+3m_2)}{4}b + \frac{m_1 m_4}{2}\right], \quad (31d)$$

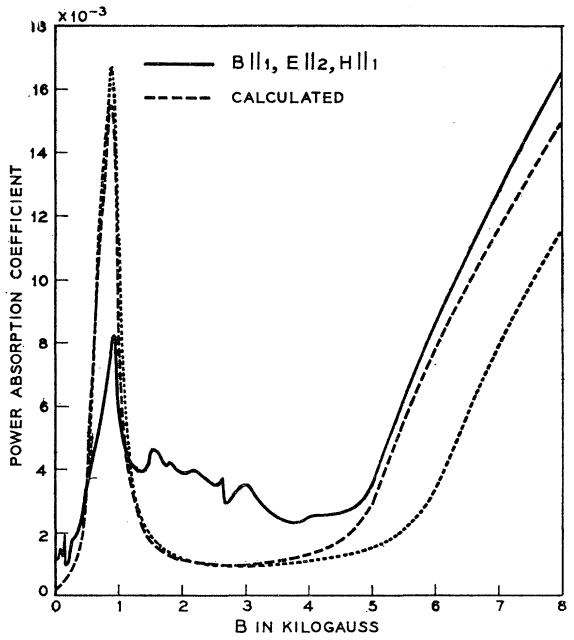

FIG. 7. Theoretical and experimental plots of power absorption coefficient as a function of magnetic field; **B** is along the binary axis and E and H refer to the polarization of the incident microwave field. The dotted curve was calculated using the electron masses quoted in reference 19 and the hole masses in reference 1.

$$\frac{\sigma_{32}}{\sigma_0}=-\frac{m_1(b+m_4)}{3\Delta_a}+\left(\frac{2}{3\Delta_c}\right)\left[\frac{m_1m_4}{2}-\frac{(m_1+3m_2)}{4}b\right], \quad (31e)$$

$$\Delta_a=m_1(m_2m_3-m_4^2+b^2), \quad (32a)$$

$$\Delta_c=m_1(m_2m_3-m_4^2)+\tfrac{1}{4}b^2(m_1+3m_2), \quad (32b)$$

where σ_0 and b are the same as for the trigonal case [Eqs. (24b) and (24c)]. Again, the hole conductivity tensor is obtained by using hole masses and changing the sign of b.

As with the trigonal case, solution of Eq. (5) for a plane wave incident shows that the normal modes for **B** parallel to axis 1 require that the electric field **E** of the incident wave be polarized either parallel or perpendicular to **B**. Again, the absorption coefficient A is given by Eq. (25).

(a.) For **E** perpendicular to **B** and along axis 2, η is given by

$$\eta^2=\epsilon_{22}-\epsilon_{23}\epsilon_{32}/\epsilon_{33}. \quad (33)$$

For **E** perpendicular to **B** and along axis 3,

$$\eta^2=\epsilon_{33}-\epsilon_{23}\epsilon_{32}/\epsilon_{33}. \quad (34)$$

The ratios of longitudinal to transverse fields are given, respectively, by

$$E_x/E_y=-\epsilon_{32}/\epsilon_{33}, \quad (35)$$

and

$$E_x/E_y=-\epsilon_{23}/\epsilon_{22}. \quad (36)$$

Since the plasma consists of two distinct types of electrons and one type of hole, there are two hybrid resonances with no resonance at the three cyclotron frequencies. One is an electron-electron hybrid, and the other is an electron-hole hybrid. A schematic plot of η^2 and the corresponding power absorption for $\omega\tau=\infty$ is shown in Fig. 2. Note the dielectric anomaly which occurs between the two hybrid resonances. For $\omega\tau=\infty$, the power absorption is zero as B is increased until the first hybrid is reached; then absorption increases with B until cutoff at the dielectric anomaly. There is no further power absorption until the second hybrid frequency is reached, whereupon power absorption increases with further increase of field.

The results for the case of **E** along axis 2 are shown in Fig. 7. The calculated position of the peak formed by the hybrid resonance at 0.5 kG and the ensuing dielectric anomaly agrees well with the observed peak, but the calculated amplitude is a factor of two larger. Using a lower relaxation time to fit the height of the peak makes the calculated shape much broader than that observed experimentally; however, the structure due to other resonances obscures the line shape at the base of the peak. Such a result is consistent with the assumption that the medium at low fields and low values of the absorption coefficient is not completely classical and that a nonlocal theory is necessary to

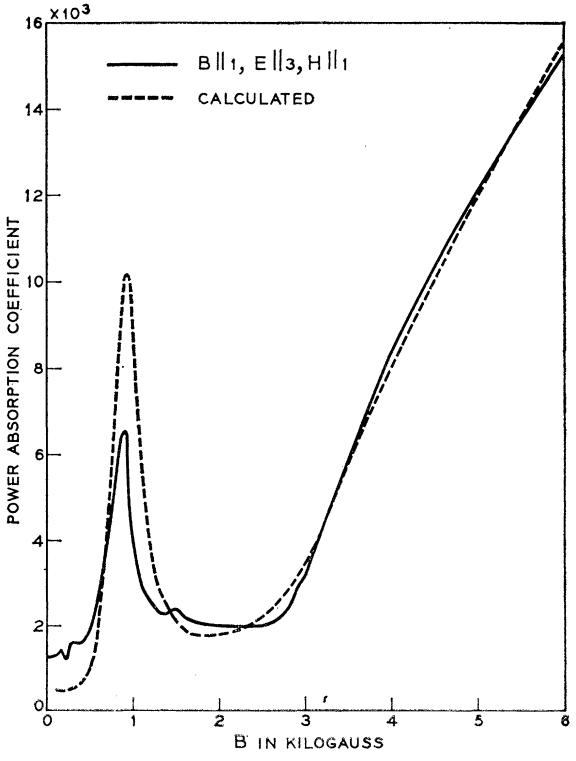

FIG. 8. Theoretical and experimental plots of power absorption coefficient as a function of magnetic field; **B** is along the binary axis and E and H refer to the polarization of the incident microwave field.

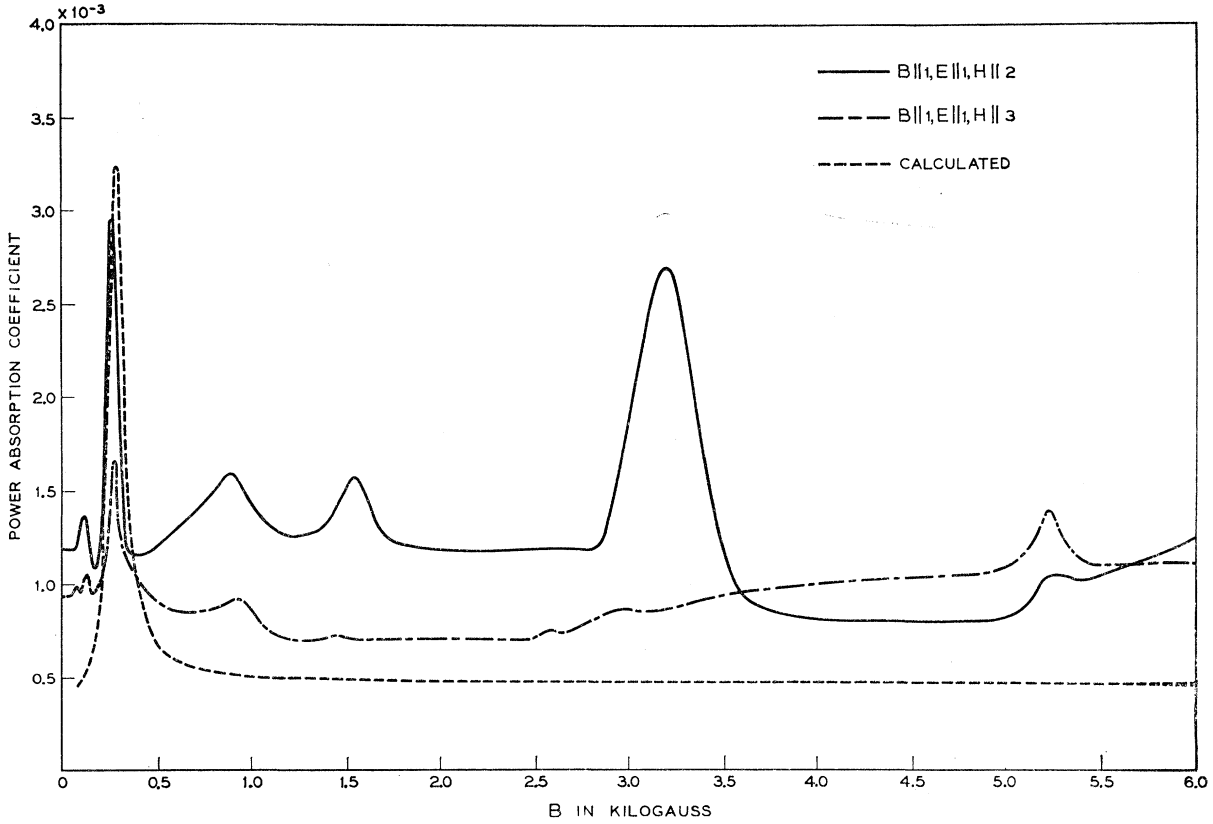

FIG. 9. Theoretical and experiment plots of power absorption coefficient as a function of magnetic field; **B** is along the binary axis and E and H refer to the polarization of the incident microwave field.

obtain an exact fit to the data. The second onset at 5.0 kG results from the electron-hole hybrid resonance; its position is very sensitive to the value of the hole effective mass.

The increase in absorption after 5.0 kG fits the calculated curve well up to about 12 kG. At larger fields (not shown in Fig. 7) the experimentally observed absorption curve bends over. We surmise that this is due to a quantum effect associated with the increase of the number of carriers which occurs when the last electron Landau level passes through the Fermi level.[14] For **B** parallel to axis 1 such crossing occurs at about 12 kG. However, for **B** parallel to axis 3 such crossing should occur for fields much greater than 17 kG because of the larger effective mass. This is consistent with the results discussed in Sec. V.A.(a), where we pointed out that the observed absorption for **B** parallel to axis 3 remained linear with B up to 17 kG.

The data shown in Fig. 8 with **E** parallel to axis 3 is similar to the case with **E** parallel to axis 2 about with the second hybrid occurring at 3.0 kG. The position of the observed peak at 900 G agrees well with the calculated peak at 950 G. Note that the sharpness of the onset of absorption at 3.0 kG indicates that a higher $\omega\tau$ should have been used, whereas the height of the peak at 900 G calls for a lower $\omega\tau$.

(b) For **E** parallel to **B**, η is given by

$$\eta^2=\epsilon_{11}. \tag{37}$$

In a manner similar to the trigonal case with **E** parallel to **B**, there is only current parallel to **B**; consequently for this orientation there are no hybrid resonances. However, there is a resonance at the cyclotron resonance for one type of electron corresponding to tilted ellipsoids b and c; it occurs for

$$eB/m_0=\omega_c=2\omega[m_1(m_2m_3-m_4^2)/(m_1+3m_2)]^{1/2}. \tag{38}$$

Even for $m_4=0$, ellipsoids b and c are tilted with respect to **B** to give tilted orbits such that there exists a component of **E** that can cause cyclotron resonance. The curves of η^2 and power absorption versus B for $\omega\tau=\infty$ are topologically similar to those in Fig. 5.

There are two experimental, and one theoretical, curves presented in Fig. 9; the calculated curve is the same whether axis 3 or axis 2 is perpendicular to the surface of the sample. The peaks associated with cyclotron resonance are observed at 260 G and 285 G for the two orientations, and the calculated peak is at 280 G. The large peak at 3.25 kG is attributed to a spin resonance of the heavy electron, and the smaller one at 5.25 kG is attributed to a hole spin resonance. Resonances evident at one half of these field values

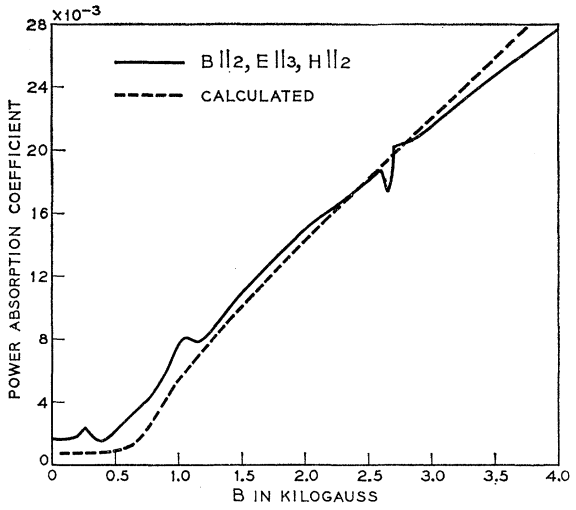

FIG. 10. Theoretical and experiment plots of power absorption as a function of magnetic field; **B** is along the bisectrix axis and E and H refer to the polarization of the incident microwave field.

are tentatively ascribed to combination resonances consisting of a spin plus cyclotron resonance transition. Low-field Azbel'-Kaner oscillations are also observed.

C. B Parallel to Bisectrix Axis

For this orientation electron ellipsoids b and c yield the same electron mass; however, their cyclotron orbits are not equivalent as a result of the tilt of the ellipsoids out of the trigonal plane ($m_4 \neq 0$). Ellipsoid a yields a distinct cyclotron mass. The conductivity tensor for electrons has the following components[17]:

$$\frac{\sigma_{11}}{\sigma_0}=\frac{(m_2m_3-m_4^2)}{3\Delta_a}+\left(\frac{2}{3\Delta_c}\right)\left[\frac{(3m_1+m_2)m_3-m_4^2}{4}\right], \tag{39a}$$

$$\frac{\sigma_{22}}{\sigma_0}=\frac{m_1m+b_3^2}{3\Delta_a}+\left(\frac{2}{3\Delta_c}\right)\left[\frac{(m_1+3m_2)m_3-3m_4^2}{4}+b^2\right], \tag{39b}$$

$$\frac{\sigma_{33}}{\sigma_0}=\frac{m_1m_2}{3\Delta_a}+\frac{2m_1m_2}{3\Delta_c}, \tag{39c}$$

$$\frac{\sigma_{13}}{\sigma_0}=\frac{\sigma_{31}}{\sigma_0}=-\left[\frac{bm_2}{3\Delta_a}+\frac{2b}{3\Delta_c}\left(\frac{3m_1+m_2}{4}\right)\right], \tag{39d}$$

$$\frac{\sigma_{12}}{\sigma_0}=\frac{\sigma_{21}}{\sigma_0}=\frac{m_4b}{3\Delta_a}-\frac{m_4b}{3\Delta_c}, \tag{39e}$$

$$\frac{\sigma_{23}}{\sigma_0}=\frac{\sigma_{32}}{\sigma_0}=-\frac{m_1m_4}{3\Delta_a}+\frac{m_1m_4}{3\Delta_c}, \tag{39f}$$

$$\Delta_a=m_1(m_2m_3-m_4^2)+m_2b^2, \tag{40a}$$

$$\Delta_c=m_1(m_2m_3-m_4^2)+\tfrac{1}{4}(3m_1+m_2)b^2, \tag{40b}$$

[17] The expression for the conductivity tensor as given in references 15 when **B** is parallel to the bisectrix axis is in error.

where σ_0 and b are the same as for the trigonal case [Eqs. (24b) and (24c)]. As before, the hole conductivity tensor is obtained by using hole masses and changing the sign of b.

Since the conductivity tensor (and, hence, the effective dielectric tensor) has all nine components different from zero, no choice of polarization of **E** of the incident wave couples to only one normal mode in the plasma for all values of B. Under such circumstances mode mixing by the sample causes both polarizations of **E** to appear in the reflected wave even though the incident wave contains only one polarization of **E**. In the calculation we assume that both polarizations can propagate freely away from the sample; in fact, one component cannot propagate in the rectangular waveguide and is, effectively, reflected back to the sample. However, such a component is small because of the large effective dielectric tensor components of the metal, which are approximately $10^6\epsilon_0$ to $10^8\epsilon_0$. Thus, the correction to the absorption coefficient from the cut-off component is small. Such an assumption is *a fortiori* justified from the over-all good fit between calculated and measured absorption curves.

Also, the solution of Eq. (5) for η, and hence, for the power absorption results in an unfactored biquadratic expression in η^2 both for **E** parallel to **B**, and **E** perpendicular to **B**. Consequently, some longitudinal electric field is always present for both orientations of **E** relative to **B**; thus there is no simple physical interpretation of the resulting resonances beyond their general character previously mentioned. However, of the two orientations, the longitudinal field is relatively weaker for **E** parallel

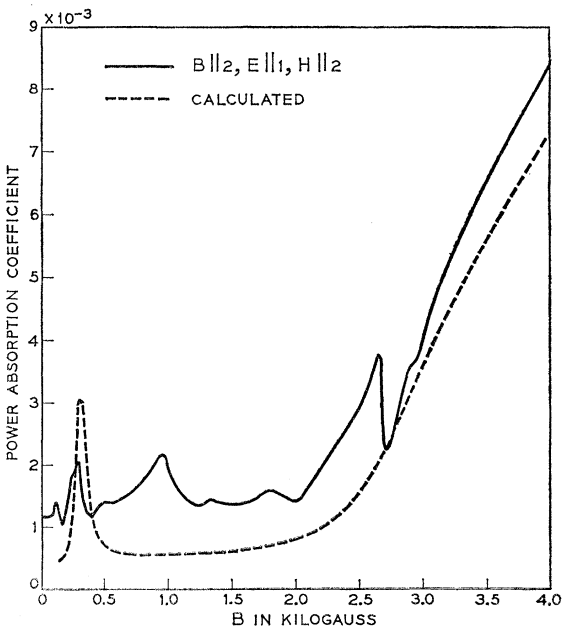

FIG. 11. Theoretical and experimental plots of power absorption as a function of magnetic field; **B** is along the bisectrix axis and E and H refer to the polarization of the incident microwave field.

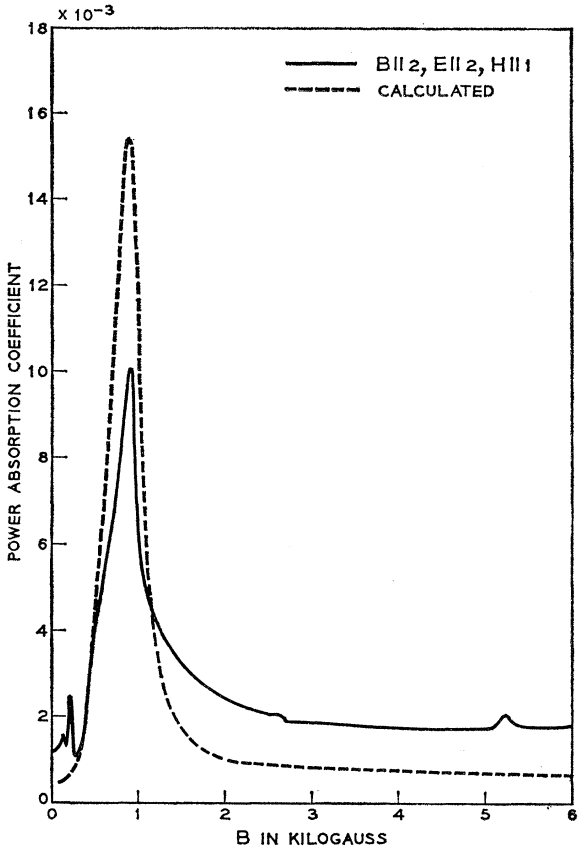

FIG. 12. Theoretical and experimental plots of power absorption as a function of magnetic field; **B** is along the bisectrix axis and E and H refer to the polarization of the incident microwave field.

to **B**. All electron orbits are tilted with respect to **B**; thus, there are resonances near the cyclotron frequencies resulting in a curve qualitatively similar to those for **B** parallel to axis 1 and axis 3. For **E** perpendicular to **B** there are two hybrid resonances (from three distinct kinds of carriers) with a dielectric anomaly in between; the power absorption curve is qualitatively similar to that of Fig. 2. The expressions for the absorption coefficient for the bisectrix case are developed in Appendix B.

The two cases for **E** perpendicular to **B** are shown in Figs. 10 and 11. In Fig. 10 where **E** is parallel to axis 3, the first hybrid at 250 G is not apparent in the calculated curve and appears only if very large values of $\omega\tau$ are used. The structure at 2.6 kG in both curves is believed to be the hole combinatorial resonance mentioned in the discussion of Fig. 9.

The results for **E** parallel to **B** are presented in Figs. 12 and 13. The two cyclotron resonance fields are at 230 G and 450 G after which there is an increase in absorption followed by a dielectric anomaly. The low-field peaks at 250 G in Figs. 12 and 13 are not apparent in the calculated curves using $\omega\tau_e=6$ and $\omega\tau_h=15$ but are barely discernible in the calculated curves using $\omega\tau_e=30$ and $\omega\tau_h=30$; one such calculated curve is shown in Fig. 13. It should be noted that the maximum absorption coefficient of 28×10^{-3} in Fig. 13 calls for a higher $\omega\tau$ than the maximum absorption value of 10×10^{-3} in Fig. 12. The small peak at 5.25 kG in both figures is again identified as a hole spin resonance, and the smaller peak at 2.6 kG in Fig. 12 is identified as a hole combination resonance.

VI. SUMMARY AND CONCLUSIONS

We have studied microwave absorption in pure bismuth with the magnetic field B in the plane of the sample along one of its crystallographic axes and with the incident microwave **E**-field polarized either perpendicular or parallel to **B**. The conditions of the experiment were such that nearly classical skin effect conditions prevailed; that is, except at low fields or whenever the experimentally observed absorption was small, the experimental results could be well fitted with a theory based on a local relationship between microwave field and current.

When **E** is perpendicular to **B** there generally exists within the bismuth plasma a longitudinal space-charge field which shields out cyclotron resonance of individual

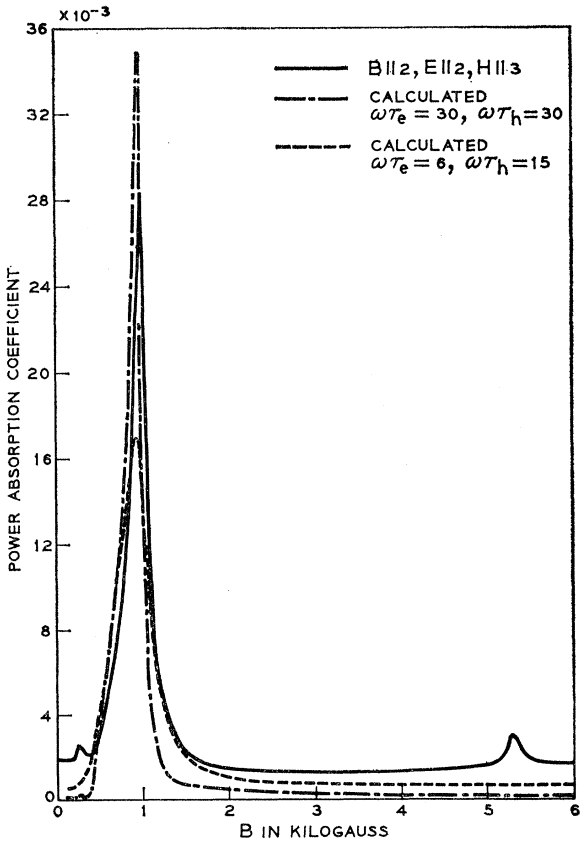

FIG. 13. Theoretical and experimental plots of power absorption as a function of magnetic field; **B** is along the bisectrix axis and E and H refer to the polarization of the incident microwave field.

carrier and which shifts the resonant frequencies to the electron-hole and electron-electron hybrid frequencies. Then, the main features of the absorption are: (1) onsets of absorption at hybrid resonance, (2) a sharp decrease of absorption at the dielectric anomaly, and (3) an increase of absorption with B at large B.

When some of the carriers are distributed among several mass ellipsoids that yield the same cyclotron mass but nonequivalent cyclotron orbits, the plasma cannot completely shield out the cyclotron resonance of such carriers. An example obtains in bismuth with **B** along the trigonal axis of the crystal; the three electron ellipsoids yield the same cyclotron mass but give elliptical orbits whose major axes are inclined at 120° to each other. For **B** along the binary axis, ellipsoids b and c yield the same cyclotron mass but equivalent orbits and ellipsoid a gives a distinct cyclotron mass; here, cyclotron resonance is completely shielded out. Finally, for **B** along the bisectrix axis, ellipsoids b and c again yield the same cyclotron mass but nonequivalent orbits because of the tilt of the ellipsoids out of the trigonal plane ($m_4 \neq 0$); the resulting cyclotron resonance is, however, obscured by mode mixing (discussed in Sec. V.C).

With **E** parallel to **B**, the E field in the plasma is mainly transverse, and cyclotron resonance absorption of individual carriers is observed only when the planes of the cyclotron orbits of carriers are tilted with respect to the magnetic field. Such tilting of orbits exists in bismuth because the electron energy ellipsoids are tilted out of the trigonal plane. The study of cyclotron resonance under such conditions is a sensitive measure of those components of the effective-mass tensor which describe the tilt.

In addition to hybrid resonances and "tilted-orbit" cyclotron resonances, we observe singularities in the absorption which we tentatively identify as either spin or combination resonances. These generally appear as a small perturbation on the general behavior of the absorption curve, and are not analyzed in detail in this paper.

We were able to fit theoretically the absorption at high fields and at the singularities in the absorption curve which we attribute either to hybrid resonance or to "tilted-orbit" cyclotron resonance. It is a general feature of the calculated absorption curves that the positions of the singularities depend on the assumed carrier masses, that the amplitudes of the various peaks and the slopes of the absorption curves at high B depend on the assumed masses and carrier concentration, and that the amplitudes and the shapes of the peaks depend on the assumed relaxation times.

Of the three parameters, masses, densities and relaxation times, it is the masses that are determined most accurately in the experiment. We obtain best fit using the following mass parameters: for electrons, $m_1=0.0062$, $m_2=1.30$, $m_3=0.017$, and $m_4=-0.085$; for holes, $M_1=0.057$, $M_3=0.77$. The electron masses quoted here are those obtained by Boyle and Brailsford[18] (except for the mass m_1 which is smaller by about 15%), and differ somewhat from those quoted by Galt[1] and by Jain and Koenig.[19] The hole mass ratio M_1/M_3 agrees with that of Galt, but the product M_1M_3 is smaller by about 20%. Our determination of M_1M_3 is based on the position of the electron-hole hybrid in Figs. 7 and 8 and is confirmed by the position of the hole spin resonance in Figs. 9, 12, and 13. Additional theoretical curves shown in Figs. 6 and 7 are examples of calculations in which hole masses of reference 1 and electron masses of reference 19 (similar to those in reference 1) were used. The lack of agreement is well outside experimental error.

In the calculation, the amplitude of the absorption is proportional to $n^{-1/2}$, where n is the carrier density. Our determination of $n=2.3\times10^{17}/\text{cm}^3$ is based on fitting the absorption coefficient, A, at high fields where classical conditions prevail; for such fitting absolute values of A are necessary. As explained in Sec. IV, absolute values of A were obtained by scaling by $\omega^{2/3}$ zero-field measurements taken in a different experiment[12] at 24 kMc/sec. This scale factor assumes that *extreme* anomalous skin effect conditions prevail at zero field. There is some doubt as to the validity of this assumption. Zero-field values measured by Aubrey[20] at 9 kMc/sec, when scaled to 24 kMc/sec, give a value of the absorption coefficient which is higher than the measured values at 24 kMc/sec. Aubrey attributes this discrepancy to relaxation effects which would also be important when scaling from 24 kMc/sec to 72 kMc/sec. If scaling by $\omega^{2/3}$ gives a value of the absorption coefficient which is too large, using a correct scaling factor would lower the absolute values of A quoted here. Therefore, a larger value of n would be necessary to fit the data and would tend to bring agreement with the value $n=4.2\times10^{17}/\text{cm}^3$ as determined optically.[18] Our determination of n accounted for the fact that the incident wave was that of TE_{01} mode of a rectangular waveguide rather than a plane wave in free space.

The theoretical curves in Figs. 4 and 6 through 13 are calculated with $\omega\tau_e=6$ and $\omega\tau_h=15$. The ratio τ_h/τ_e is that used to fit low-field galvanomagnetic experiments.[21] The magnitudes of $\omega\tau_e$ and $\omega\tau_h$ are a compromise choice. We have tried both higher and lower values of $\omega\tau$ and different $\omega\tau$'s for each distinct electron ellipsoid. No choice of $\omega\tau$'s gives complete agreement with experiment. Higher $\omega\tau$'s give better fit to the sharpness of the absorption peaks and of the onsets of absorption. Lower $\omega\tau$'s give better agreement with the heights of the absorption peaks near the dielectric anomalies. We surmise that the carriers in our samples have relaxation times longer than those used in the calculation, but that there exists near a dielectric

[18] W. S. Boyle and A. D. Brailsford, Phys. Rev. **120**, 1943 (1960).
[19] A. L. Jain and S. H. Koenig, Phys. Rev. **127**, 442 (1962).
[20] J. E. Aubrey, J. Phys. Chem. Solids **19**, 321 (1961).
[21] R. N. Zitter, Phys. Rev. **127**, 1471 (1962).

anomaly some additional damping mechanism, not accounted for by a simple, field-independent relaxation time. Such damping may originate from excitation of plasma oscillations[22] or from Landau damping.[23] In addition, there is lack of agreement wherever the experimentally measured absorption is low. There, a theory which is based on local relationship between current and field is not adequate because the skin-effect conditions are somewhat anomalous. Under such circumstances the measured absorption should be greater than that calculated; such is the case in the data in nearly all the figures. However, when the absorption coefficient becomes large as B increases, the skin depth becomes large, and the cyclotron radius becomes small; then classical conditions prevail and and the fit becomes very good. *Note added in proof.* It has been proposed [for example, see B. Lax, J. G. Mavroides, H. J. Zeiger and R. J. Keyes, Phys. Rev. Letters **5**, 241 (1960)] that the conduction band in Bi is not parabolic as indicated by Eq. (19) but is given by

$$E(1+E/E_g)=(\hbar^2/2m_0)\mathbf{k}\cdot\boldsymbol{\alpha}\cdot\mathbf{k}.$$

Some recent work by R. N. Brown, J. G. Mavroides, and B. Lax (to be published) on infrared magneto-reflection in bismuth is consistent with this model, and they obtain values of $E_g=15$ MeV for the band gap, and $E_F=25$ MeV for the Fermi energy. The previously assumed values were $E_g=50$ MeV and $E_F=18$ MeV. Using the new values of E_F and E_g, one calculates the number of carriers (electrons or holes) to be 2.4×10^{17}/cm^3 in good agreement with our value of 2.3×10^{17}/cm^3 and Zitter's[21] value of 2.5×10^{17}/cm^3.

ACKNOWLEDGMENTS

We wish to thank Dr. W. S. Boyle, Dr. J. K. Galt, and Dr. P. A. Wolff for many stimulating discussions, J. M. Olson for technical assistance, and J. J. Schott for growing crystals.

APPENDIX A

We wish to show how, when a high-density plasma possesses anisotropic carriers of cyclotron mass m^*, cyclotron resonance of such carriers is shielded out for for the extraordinary wave when the carriers are given by a single mass tensor, but that it is not shielded out when the carriers are distributed among two (or more) nonequivalent mass tensors.

To prove the first contention, assume without loss of generality that the plasma contains anisotropic electrons whose effective mass tensor is given by

$$\mathfrak{m}=m_0\begin{bmatrix} m_1 & 0 & 0 \\ 0 & m_2 & 0 \\ 0 & 0 & m_3 \end{bmatrix}, \tag{A1}$$

and that the static magnetic field is along axis 3. From the equations of motion of such electrons

$$\mathfrak{m}\cdot\partial\mathbf{v}/\partial t=-e\mathbf{v}\times\mathbf{B}, \tag{A2}$$

it follows that the cyclotron frequency is $eB/[m_0(m_1m_2)^{1/2}]$, so that the cyclotron mass is

$$m^*=m_0(m_1m_2)^{1/2}.$$

The cyclotron orbit is an ellipse with a right-handed sense with the eccentricity (ratio of x to y axis) given by $(m_2/m_1)^{1/2}$.

The contribution of such electrons to the plasma conductivity tensor is

$$\boldsymbol{\sigma}=(\sigma_0/\Delta)\begin{bmatrix} m_2 & b & 0 \\ -b & m_1 & 0 \\ 0 & 0 & \Delta/m_3 \end{bmatrix}, \tag{A3}$$

where in the limit of infinite relaxation time, $\sigma_0=ne^2/jm_0\omega$; $b=-eB/jm_0\omega$ and $\Delta=m_1m_2+b^2$. The polarization of the extraordinary wave propagating in the x direction is given by $E_x/E_y=-\epsilon_{xy}/\epsilon_{xx}$ where $\boldsymbol{\varepsilon}$, the dielectric coefficient of the plasma, is given in terms of the total plasma conductivity tensor $\boldsymbol{\sigma}_T$, $\boldsymbol{\varepsilon}=\mathbf{I}+\boldsymbol{\sigma}_T/j\omega\epsilon_0$. In general, the polarization of the extraordinary wave depends on all carriers, but near $\Delta=0$ it is given by

$$\frac{E_x}{E_y}=-\frac{\sigma_{xy}}{\sigma_{xx}}=-\frac{b}{m_2}\bigg|_{b=j(m_1m_2)^{1/2}}=-j\left(\frac{m_1}{m_2}\right)^{1/2}. \tag{A4}$$

Thus, at electron cyclotron resonance the field is elliptically polarized in the left-handed sense and with the eccentricity inverse of that of the electron cyclotron orbit. Thus, its polarization is precisely orthogonal to that required to excite cyclotron resonance with the consequence that the propagation constant of the extraordinary wave exhibits no cyclotron resonance.

To prove the second contention, assume that the anisotropic electrons of cyclotron mass $m^*=m_0(m_1m_2)^{1/2}$ are distributed between the two ellipsoids $\mathfrak{m}_\alpha$ and $\mathfrak{m}_\beta$,

$$\begin{aligned}\mathfrak{m}_\alpha&=m_0\begin{bmatrix} m_1 & 0 & 0 \\ 0 & m_2 & 0 \\ 0 & 0 & m_3 \end{bmatrix},\\ \mathfrak{m}_\beta&=m_0\begin{bmatrix} m_2 & 0 & 0 \\ 0 & m_1 & 0 \\ 0 & 0 & m_3 \end{bmatrix}.\end{aligned} \tag{A5}$$

The β ellipsoid can be obtained by rotating the α ellipsoid by $\pi/2$. The cyclotron orbits of the α and β electrons are right-handed ellipses with eccentricities (ratio of x to y axis) of $(m_2/m_1)^{1/2}$ and $(m_1/m_2)^{1/2}$, respectively. The contribution of such electrons to the plasma conductivity tensor is

$$\boldsymbol{\sigma}=(\sigma_0/2\Delta)\begin{bmatrix} m_1+m_2 & 2b & 0 \\ -2b & m_1+m_2 & 0 \\ 0 & 0 & 2\Delta/m_3 \end{bmatrix}. \tag{A6}$$

[22] H. Fröhlich and H. Pelzer, Proc. Phys. Soc. (London) **A68**, 525 (1955).

[23] L. D. Landau, J. Phys. (USSR) **10**, 25 (1946); J. D. Jackson, J. Nucl. Energy Part C, **1**, 171 (1960).

The polarization of the extraordinary wave at $\Delta=0$ is again

$$\frac{E_x}{E_y}=-\frac{\sigma_{xy}}{\sigma_{xx}}=-\frac{2b}{(m_1+m_2)}\Bigg|_{b=j(m_1m_2)^{1/2}}$$

$$=-2j\frac{(m_1m_2)^{1/2}}{(m_1+m_2)}. \quad \text{(A7)}$$

At cyclotron resonance the field rotates in the left-hand sense but is of the wrong eccentricity to be orthogonal to either the α- or β-electron orbits. Consequently, there exists a component of the field that can excite cyclotron resonance in this case.

APPENDIX B

When **B** is parallel to the bisectrix axis, the absorption coefficient is derived as follows. Let η_{1k}, $k=1, 2$, be the two roots in the fourth quadrant of

$$\eta_{1k}^4-B_1\eta_{1k}^2+C_1=0, \quad \text{(B1)}$$

where

$$C_1=(\det\epsilon)\epsilon_{33} \quad \text{(B2)}$$

and

$$B_1=\epsilon_{11}+\epsilon_{22}-(\epsilon_{13}\epsilon_{31}+\epsilon_{23}\epsilon_{32})/\epsilon_{33}. \quad \text{(B3)}$$

Define

$$G_{1k}=\frac{\epsilon_{33}(\epsilon_{11}-\eta_{1k}^2)-\epsilon_{13}\epsilon_{31}}{\epsilon_{12}\epsilon_{33}-\epsilon_{13}\epsilon_{32}}; \quad k=1, 2. \quad \text{(B4)}$$

Also, let η_{3k}, $k=1, 2$, be the two roots in the fourth quadrant of

$$\eta_{3k}^4-B_3\eta_{3k}^2+C_3=0, \quad \text{(B5)}$$

where

$$C_3=(\det\epsilon)/\epsilon_{11} \quad \text{(B6)}$$

and

$$B_3=\epsilon_{22}+\epsilon_{33}-(\epsilon_{12}\epsilon_{21}+\epsilon_{13}\epsilon_{31})/\epsilon_{11}. \quad \text{(B7)}$$

Define

$$G_{3k}=\frac{\epsilon_{11}(\epsilon_{33}-\eta_{3k}^2)-\epsilon_{13}\epsilon_{31}}{\epsilon_{11}\epsilon_{32}-\epsilon_{12}\epsilon_{31}}, \quad k=1, 2. \quad \text{(B8)}$$

To denote the solutions for the electric fields from the cofactors of Eq. (5), three indices are required: $E_{ij,\alpha}$ will denote the αth component of the reflected electric field vector where i denotes the sample axis parallel to the incident microwave **E** vector and j denotes the sample axis parallel to the incident microwave **H** vector; either vector can be parallel to **B**. Then using $i=1, 3$ and $j=1, 3$ *only*, the solutions for the electric field components, reflection coefficients, R_{ij}, and absorption coefficients, A_{ij}, can be expressed as follows: Let

$$D_j=(1+\eta_{j1})(1+\eta_{j2})(G_{j1}-G_{j2}); \quad \text{(B9)}$$

then

$$E_{j2,y}=(1/D_j)[(G_{j1}-G_{j2})(\eta_{j1}\eta_{j2}-1)-(G_{j1}+G_{j2})(\eta_{j1}-\eta_{j2})], \quad \text{(B10)}$$

$$E_{j2,z}=(1/D_j)[-2G_{j1}G_{j2}(\eta_{j1}-\eta_{j2})]; \quad \text{(B11)}$$

$$R_{j2}=|E_{j2,y}|^2+|E_{j2,z}|^2, \quad \text{(B12)}$$

$$A_{j2}=1-R_{j2}. \quad \text{(B13)}$$

$$E_{2j,y}=(2/D_j)(\eta_{j1}-\eta_{j2}), \quad \text{(B14)}$$

$$E_{2j,z}=(1/D_j)[(G_{j1}-G_{j2})(\eta_{j1}\eta_{j2}-1)+(G_{j1}+G_{j2})(\eta_{j1}-\eta_{j2})]; \quad \text{(B15)}$$

$$R_{2j}=|E_{2j,y}|^2+|E_{2j,z}|^2, \quad \text{(B16)}$$

$$A_{2j}=1-R_{2j}. \quad \text{(B17)}$$